

## Rotor Flux Controller for Induction Machines Considering Main Inductance Saturation

**Diachenko G.**  
Dnipro University of Technology  
Dnipro, Ukraine

**Abstract.** This paper discusses the problem of controlling electromechanical systems with maximum performance while maintaining accuracy and minimum power consumption. The objective of the study is to develop a law for regulating the coordinates of an electromechanical system, taking into account an energy-efficient algorithm for transferring the system from one operation point to another. An essential feature of the proposed solution is the possibility of applying the approach in modern high-speed electromechanical systems operating mainly in transient modes, without providing additional requirements for the digital part. The objective is achieved through the use of the law of the rotor flux generation augmented with adaptive low-pass filtering of the flux reference at each sampling step. The proposed method is investigated in both steady-state and dynamic modes of operation using laboratory experiments with a 370-W induction machine. With appropriate control of the change rate of the magnetic flux, the losses during the full operating cycle with changes in the torque can be significantly reduced compared to the conventional approach. The varying load is typical for the electromechanical systems with a variable moment of inertia and requirements for the positioning accuracy. The most critical result of the study is the reduction of the minimum possible cycle time, at which the expediency of using loss-minimizing control methods remains actual. The significance of the results obtained is in the reduction of losses while maintaining the required torque, contributing to the more efficient operation of this machine type.

**Keywords:** dynamic operation, energy efficiency, induction machine, optimization, adaptive filtering.

**DOI:** 10.5281/zenodo.4018933

**UDC:** 681.518

### Fluxul magnetic optim și reducerea valorii minime a ciclului în problemele de dirijarea energoeficiente cu mașina electrică.

**Deacenko G.G.**  
Politehnica Dnipro,  
Dnipro, Ucraina

**Rezumat.** În această lucrare s-au analizat posibilele opțiuni pentru formarea legilor de control al curentului (fluxului magnetic) al unei mașini electrice, luând în considerare constrângerile cunoscute anterior pentru realizarea acestor opțiuni. O caracteristică importantă a soluției propuse în lucrare este posibilitatea aplicării legii propuse în sistemele electromecanice moderne de mare viteză care funcționează în principal în regimuri tranzitorii, fără a prevedea cerințe suplimentare pentru partea digitală. S-a utilizat un model dinamic în spațiul de stare aplicat în contextul de minimizare a pierderilor de putere a sistemului de control a mașini electrice de curent alternativ. Pe baza funcției de pierdere, care ia în considerare regimurile de funcționare statice și dinamice ale acționării electrice, se propune o abordare a utilizării metodei de poziționare, care conduce la minimizarea valorilor fluxului magnetic la fiecare pas de discretizare. În regim de funcționare intermitentă a motorului cu frânare electrică și cu influența proceselor de pornire cu umplerea de 60%, metoda propusă rămâne operațională. Rezultatele prezentate pentru cazul unei traiectorii cunoscute anterior a modificării cuplului electric al motorului fac posibilă reducerea în continuare a pierderilor de putere în comparație cu cazul valorilor necunoscute în avans. Acest lucru, la rândul său, duce la diminuare a duratei ciclului minim de timp posibil de funcționare într-un regim intermitent pentru care se păstrează oportunitatea utilizării metodelor de control eficiente din punct de vedere energetic.

**Cuvinte-cheie:** mașină electrică, control, eficiență energetică.

### Регулятор магнитного потока ротора асинхронного двигателя с учетом насыщения магнитопровода

**Дяченко Г. Г.**  
Национальный технический университет «Днепровская политехника»  
Днепр, Украина

**Аннотация.** В работе решается задача управления электромеханическими системами, обладающими максимальным быстродействием при одновременном сохранении точности и минимальным

энергопотреблением. Цель работы заключается в разработке закона управления координатами электромеханической системы с энергоэффективным алгоритмом перевода из одной рабочей точки в другую. Важной особенностью предложенного в работе решения, является возможность применения предложенного закона в современных быстродействующих электромеханических системах, работающих преимущественно в переходных режимах, не предусматривая дополнительных требований к цифровой части. Поставленная цель достигается путем использования закона формирования потока ротора асинхронного двигателя с адаптивной фильтрацией уставки магнитного потока на каждом шаге дискретизации. Эффективность предложенного решения была исследована с помощью лабораторных экспериментов с машиной переменного тока мощностью 370 Вт как статическом, так и в динамическом режимах работы. Показано, что при соответствующем управлении скоростью изменения магнитного потока потери за полный рабочий цикл при изменениях крутящего момента могут быть уменьшены по сравнению с классическим подходом. Потери в установившемся режиме значительно уменьшаются в сравнении с удержанием магнитного потока на номинальном уровне при варьировании нагрузки в широком диапазоне, что характерно для электромеханических систем с переменным моментом инерции, к которым одновременно выдвигаются требования по точности позиционирования. В повторно-кратковременном режиме работы двигателя с электрическим торможением и влиянием пусковых процессов при скважности 60% метод сохраняет свою работоспособность. Наиболее существенным результатом работы является уменьшение минимально возможного времени цикла работы в повторно-кратковременном режиме, при котором сохраняется целесообразность использования методов энергоэффективного управления. Значимость полученных результатов состоит в уменьшении потерь при сохранении необходимого крутящего момента, что способствует более эффективной работе электрических машин данного типа.

**Ключевые слова:** динамический режим, энергоэффективность, асинхронная машина, оптимизация, адаптивная фильтрация.

## INTRODUCTION

Modern technological processes of packaging, machining and sorting can be implemented in various operations. Electromechanical systems servicing such technological processes operate in the transient modes most of the time to secure maximum productivity. The advancement of a semiconductor technology and microprocessor devices [1], [2] extends the feasibility of designing and creating highly dynamic drives for the electromechanical systems. Simultaneously with a power consumption decrease, there is an increasingly compelling task to enhance precision in dynamic modes of operation. The most promising challenge is the creating of electromechanical systems with a supreme performance while preserving accuracy and minimum energy loss [3]. Rational energy management is provided by the design features of electrical machines, electronics solutions of the converters, and a new semiconductor component base. An increase in digital device performance has formed the prospects for the development of the creation of control systems. The control systems provide the generation of a control trajectory according to complex algorithms that take into account many factors [4], [5]. Thus, a critical task is the development of the laws for ensuring a rational transfer of an electromechanical system from one steady-state working point to the desired point along a

trajectory that provides maximum speed and minimizes the energy loss, while simultaneously meeting a minimum of these two factors.

The efficient and cost-effective drive is also a vital requirement for electric vehicles and automated manufacturing [6-9]. High efficiency can be obtained by exploiting a permanent magnet or separately excited synchronous motors. However, the use of these "cool toys" sure comes at a price, as the manufacturing of the permanent magnets from the high-cost rare earth elements is required. In contrast, induction machines come up with an excellent robustness, a low cost, and a simple structure. Despite the advantages listed, the efficiency of the induction machines is smaller and decreases even more when operated in part-loaded modes. Thus, the critical reason for solving the energy efficiency issue of this machine type is an eager desire to make them more attractive than the synchronous machines.

Many scientific publications and technical reports addressed the aforementioned problem for the steady-state operation of the induction machine for different applications [10-12]. Yet, in the applications such as an electric vehicle, autonomous robots and other electromechanical systems with a variable moment of inertia with the strict positioning requirements, motors are regularly run in dynamic mode with frequently changing torque and speed up to the current and voltage limits. Consequently, an appropriate

control system is required to fully experience all the benefits of using an induction machine in such applications. One of the earliest treatments of this question is examined in [13]. The submitted offline solution for a definite set of operating situations has provided a significant advance compared to the constant flux mode. A predictive method utilizing a parametrized approximating curve is given in [14]. The paper [15] discusses the development of such parametrized trajectories but without analyzing the voltage and the current boundary conditions. A suboptimal solution in the form of a relationship between the stator field-producing current and the torque-producing current based on a look-up table with precalculated data points is presented in [16]. However, it is a troublesome activity to obtain such a look-up table with the desired accuracy for various types of machines, especially when the saturation effects of the main inductance must be taken into consideration. An analytical solution of the dynamic optimization problem of the induction machines is presented in [17]. The nonlinearities were neglected due to the main inductance saturation. Ranta et al. [18] applied a search method to a corresponding function of a power loss. The returned value was then applied to the control scheme through the filter to reduce power loss peaks during the transients. Although the filter has been used, no details have been given. Neither the appropriate choice of the filter type nor the time constant has been discussed. This concept was further numerically investigated in [19] regarding both the appropriate filter type and loss-minimizing filter coefficients. The analysis was conducted for three induction motors with different rated powers. However, the saturation effect was neglected, and the found value of the appropriate filter's coefficient remained constant for all torque profiles. These issues were addressed later in [20], but the practical implementation was not provided. Besides, all the reviewed methods apply a loss-minimizing reference while applying the torque. Such a solution always leads to a power loss increase compared to operation at a constant flux reference during the transients. Hence a control system must be provided with reliably predicted values of the future torque profile. With this information, it is possible to further reduce energy losses in the drive applications with heavy torque dynamics.

In this paper, the described in [20] is applied as a loss-minimizing control. The model

accounts for the main inductance saturation. A minimizing flux reference and filter coefficient are found at each sampling step based on the corresponding power loss function. The steady-state and dynamic performance of the proposed method is investigated using laboratory experiments with a 370-W induction motor. The current paper also covers the situation when the future load profile is known. The control system can dynamically adapt the flux before there is a demand for a different torque level.

The paper is organized as follows. The following three subsections *A*, *B* and *C* describe the motor model, the main inductance saturation curve and the model of losses in induction machines used in this paper. Then, in subsection *D*, the control problem is formulated. Finally, subsection *E* illustrates the results of laboratory experiments.

## METHODS, RESULTS AND DISCUSSION

### A. Motor model

The motor model parameters used in the sequel are the parameters of the  $\Gamma$ -inverse equivalent circuit shown in Fig. 1 following the representation from [21], where  $\omega_1$  is the angular frequency of the stator field,  $\underline{U}_1$  is the stator voltage phasor,  $\underline{I}_1$  and  $\underline{I}_2$  are the stator and rotor current phasors,  $R_1$  and  $R_2$  are the stator and rotor resistances, respectively,  $L_\sigma$  is the stray inductance, and lastly,  $L_m$  is the main inductance.

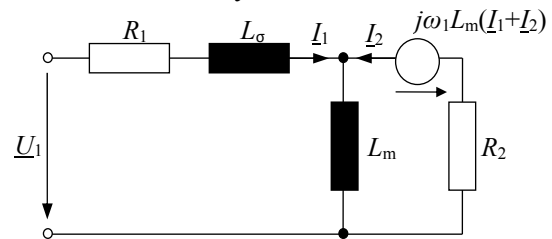


Fig. 1.  $\Gamma$ -inverse equivalent circuit of an induction machine.

An induction machine used for high dynamics applications is typically controlled in a field-oriented scheme. The approach in this paper implies the field orientation along the rotor flux linkage  $\Psi_2$ , i.e., the flux linkage is aligned with the d-axis of the rotating coordinate frame. The dynamics of the currents, flux linkage, and rotor speed are given as a continuous state-space model

$$\begin{cases} \dot{x} = A(x)x + Bu + \delta \\ y = Cx \end{cases} \quad (1)$$

with states  $x \in \mathbb{R}^{(4 \times 1)}$  as  $x = [i_{1d} \ i_{1q} \ \Psi_2 \ \omega_2]^T$  and controls  $u \in \mathbb{R}^{(2 \times 1)}$  as  $u = [u_{1d} \ u_{1q}]^T$ ;  $\delta \in \mathbb{R}^{(4 \times 1)}$  is given by  $\delta = [0 \ 0 \ 0 \ Z_p(T_e - T_L)J^{-1}]^T$ , where  $J$  is the total moment of inertia,  $Z_p$  is the number of pole pairs,  $T_e$  and  $T_L$  are the motor and load torques.  $A(x) \in \mathbb{R}^{(4 \times 4)}$  represents the characteristic matrix of the dynamic system

$$A = \begin{bmatrix} -(R_1 + R_2)L_\sigma^{-1} & \omega_1 & R_2L_m^{-1}L_\sigma^{-1} & 0 \\ -\omega_1 & -R_2L_\sigma^{-1} & -\omega_1L_\sigma^{-1} & 0 \\ R_2 & 0 & -R_2L_m^{-1} & 0 \\ 0 & 0 & 0 & 0 \end{bmatrix} \quad (2)$$

with  $\omega_1$  representing the synchronous speed in electrical radians per second.  $B \in \mathbb{R}^{(4 \times 2)}$  is the input matrix given by

$$B = \begin{bmatrix} L_\sigma^{-1} & 0 \\ 0 & L_\sigma^{-1} \\ 0 & 0 \\ 0 & 0 \end{bmatrix}. \quad (3)$$

$y \in \mathbb{R}^{(2 \times 1)}$  is the outputs vector; the matrix of the outputs  $C \in \mathbb{R}^{(2 \times 4)}$  in the current study is represented by

$$C = \begin{bmatrix} 0 & 0 & 1 & 0 \\ 0 & 0 & 0 & 1 \end{bmatrix}. \quad (4)$$

The following expression gives the electromagnetic torque

$$T_e = \frac{3}{2} Z_p \Psi_2 i_{1q}. \quad (5)$$

### B. Main inductance saturation

In practice, the modeling of an induction machine as a linear object is inadequate even for the nominal mode of operation. Thus, the model of an induction machine must take into account the effects of magnetic saturation [22]. The dependency of the main inductance  $L_m$  on the field-producing current  $i_{1d}$  is considered as illustrated in Fig. 2 for the motor under test covered in this paper.

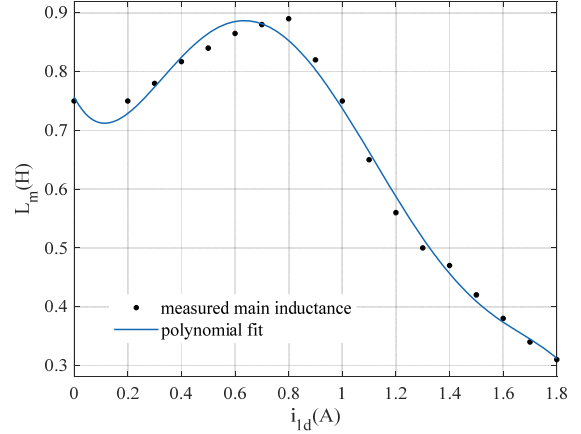


**Fig. 2. Polynomial approximation of the main inductance curve as a function of the field-producing current for a 370-W motor. Markers show the measured inductance values from the tests.**

The main inductance data points  $L_m(i_{1d}): \mathbb{R} \rightarrow \mathbb{R}, \forall i_{1d} \in \mathbb{R}$  are obtained from the measurements using laboratory testbench described in the experimental setup subsection and fitted to the 5<sup>th</sup> order polynomial function using the Curve Fitting Toolbox of MATLAB, resulting in the next expression

$$L_m(i_{1d}) = \sum_{n=1}^{k=6} P_n i_{1d}^{k-n}. \quad (6)$$

Consequently, the steady-state rotor flux is given by  $\Psi_2 = L_m(i_{1d}) \cdot i_{1d}$ , and the rotor time constant is calculated from  $T_2 = L_m(i_{1d}) \cdot R_2^{-1}$ .

### C. Losses

The input power is the sum of the output mechanical power  $P_{out}$  and the power loss  $P_{loss}$

$$P_{in} = P_{out} + P_{loss} = \omega(t)T_e(t) + P_{loss}. \quad (7)$$

The focus of this paper is the copper losses. The core losses are not taken into consideration due to the fact that they are being indirectly reduced through the loss-minimizing flux level control. Moreover, the inclusion of the core losses is usually done at the expense of the higher computational requirements for the digital part. Using the amplitude invariant scaling of the Clarke transform and the Park transform for the currents and voltages, the instantaneous power losses  $P_{loss}$  in the induction machine, directly from the equivalent circuit in Fig. 1, are given by

$$P_{loss} = \frac{3}{2} R_1 (i_{1d}^2 + i_{1q}^2) + \frac{3}{2} R_2 (i_{2d}^2 + i_{2q}^2), \quad (8)$$

where  $i_{1d}$ ,  $i_{1q}$  and  $i_{2d}$ ,  $i_{2q}$  are the stator current and rotor current phasor components under a rotor flux phasor orientation, respectively. The components  $i_{2d}$ ,  $i_{2q}$  of the rotor phasor can be obtained after some mathematical operations as follows

$$\begin{aligned} i_{2d} &= \Psi_2 L_m^{-1} (i_{1d}) - i_{1d} = \Psi_2 R_2^{-1} \\ i_{2q} &= -i_{1q} \end{aligned} \quad (9)$$

Substitution of (9) into (8) results in

$$\begin{aligned} P_{loss} &= \frac{3}{2} R_1 (i_{1d}^2 + i_{1q}^2) + \frac{3}{2} R_2 (i_{1d}^2 + i_{1q}^2) \\ &+ \frac{3}{2} R_2 \left( \frac{1}{L_m^2 (i_{1d})} \Psi_2^2 - \frac{2}{L_m (i_{1d})} \Psi_2 i_{1d} \right). \end{aligned} \quad (10)$$

The power loss  $P_{loss}$  in (10) include both a constant power loss in the steady-state mode of operation and a transient power loss in the dynamic mode of operation.

#### D. Control problem formulation

The objective of this paper is to regulate the coordinates of an electromechanical system in a dynamic operation (for changing load torques and/or changing speeds) as energy-efficient as possible. That is, to transfer the electromechanical system with the motor torque  $T_e$  from one steady-state operation point  $T_0$  to another point  $T_1$  with minimal losses over the duty cycle. The speed reference in the form of a speed profile  $\omega_{2,ref}(t)$  is in the time interval  $t \in [t_0 \ t_f]$ . In contrast to the loss-minimizing control methods that consider solely the steady-state modes of operation, the power losses will not have a constant value within the considered time interval. Hence, the overall efficiency must be calculated based on the total energy losses. The performance index is formulated as follows

$$J = \int_{t_0}^{t_f} P_{loss}(t) dt. \quad (11)$$

The performance index  $J$  from (11) represents the power losses solely from (10) as the main minimization priority with no account for a possible speed deviation from the reference trajectory.

The control is implemented by considering the flux dynamics augmented with low-pass filtering

$$\dot{\Psi}_2(t) = [\Psi_{2,ref}(t) - \Psi_2(t)] T_\Psi^{-1}, \quad (12)$$

where  $T_\Psi$  is the time constant of the low-pass filter. Also, the equality constraint with respect to the torque  $T_e$  from (5) and the inequality constraints (13) and (14) are taken into account

$$\sqrt{u_{1d}^2 + u_{1q}^2} \leq V_s, \quad (13)$$

$$\sqrt{i_{1d}^2 + i_{1q}^2} \leq I_s. \quad (14)$$

$V_s$  is the maximum length of the inverter output voltage phasor, which depends on the DC link voltage of the inverter.  $I_s$  represents both the maximum length of the inverter output current phasor or the current limitation of the considered electric machine. Any additional constraints, e.g., concerning the upper or lower terminal values of the state variables, can be imposed if appropriate.

The system dynamics (1) and (12) as well as the constraints (13) and (14) will be solved numerically due to the nonlinear nature of the objective functional (11). This needs to be done to find the value of the filter time constant corresponding to the minimal energy loss during the transient. The general formulation of the search of the loss-minimizing value of the rotor flux is shown below

$$\begin{aligned} \Psi_{2,ref} &= \arg \min_{\Psi_2 \in [\Psi_{2,min}, \Psi_{2,max}]} \{P_{loss}(\Psi_2)\} \end{aligned} \quad (15)$$

The minimum point of the performance objective functional (11) is found by means of a 1-D golden section method at each sampling period. Then, the found value is low-pass filtered. The convergence of the search method to a local minimum is proved in [20] using the Lyapunov function. For the implementation purposes, the continuous-time system dynamics (1) – (5) is represented in the discrete-time system with the sample time  $T_s$  and  $t = kT_s$ . Hence, the discrete-time version of the objective functional (11) looks as follows

$$J_d = \sum_{k=1}^N P_{loss}(k), \quad (16)$$

where  $P_{\text{loss}}(k)$  is the discretized function of a power loss (10) at the sampling instants. Substituting (10) in (16) results in

$$\begin{aligned}
 J_d = & \frac{3}{2} R_1 \sum_{k=1}^N i_{1d}^2(k) + \\
 & \frac{2}{3} (R_1 + R_2) Z_p^{-2} \sum_{k=1}^N T_e^2(k) \Psi_2^{-2}(k) + \\
 & \frac{3}{2} R_2 \sum_{k=1}^N \left( i_{1d}^2(k) + L_m^{-2} (i_{1d}(k)) \Psi_2^2(k) \right) - \\
 & 3 R_2 \sum_{k=1}^N L_m^{-1} (i_{1d}(k)) i_{1d}(k) \Psi_2(k)
 \end{aligned} \quad (17)$$

The state discretization is implemented using the forward Euler method.

### E. Experimental setup

The control problem formulation from the previous section is now investigated in both steady-state and dynamic modes of operation using the test bench illustrated in Fig. 3.

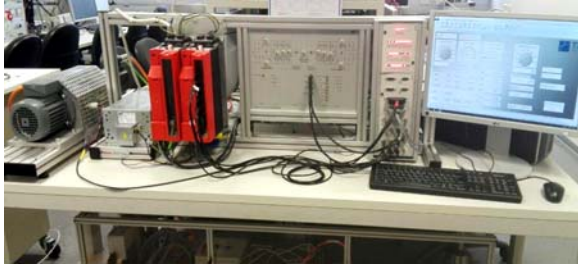


Fig. 3. Test bench.

A 370-W induction machine is used in laboratory experiments. The rated values of the considered machine are given in Table 1.

Table 1

Motor data

$R_1$	27.8 $\Omega$	$R_2$	20 $\Omega$
		$L_\sigma$	0.142 H
$Z_p$	2	$J$	$22 \cdot 10^{-4}$ kgm <sup>2</sup>
$P_1$	-0.669	$P_2$	3.606
$P_3$	-6.622	$P_4$	4.415
$P_5$	-0.743	$P_6$	0.754
		$T_N$	2.59 Nm
$\omega_{2,1}$	20.94 rad/s (200 rpm)	$\omega_{2,2}$	104.7 rad/s (1000 rpm)

The induction machine is powered by a SEW-Eurodrive frequency converter controlled by a dSPACE DS1104 R&D controller board in all experiments. The controller hardware in the inverter is bypassed to access the PWM-signals of the power stage as well as the internal current and dc-link-voltage sensors. In all tests, a permanent magnet synchronous machine is used

as a load provider. A standard inverter controls the synchronous machine. The torque is measured using the KTR Dataflex 22/20 torque sensor.

Figure 4 shows the measured losses as a function of the field-producing current.

Five different shaft torque values were applied. It can be seen that measured losses depend on the field-producing current (flux). It can also be noticed that losses are minimized by appropriately selecting the field-producing current (flux level).

Likewise, the loss-minimizing flux level was found for each torque using (15). Data points from (15) agree well with the actual loss-minimizing values.

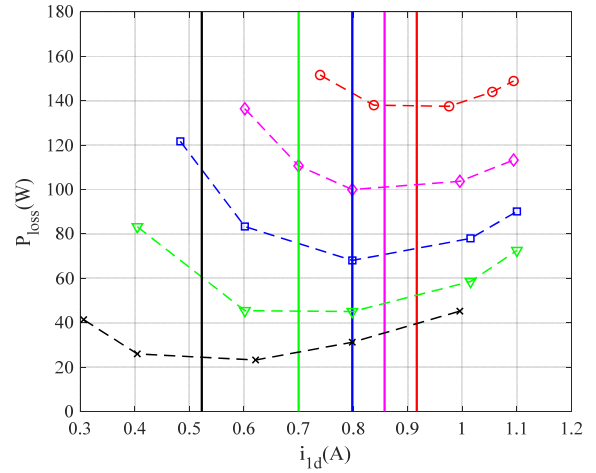


Fig. 4. Measured losses (markers) as a function of the field-producing current and corresponding theoretical optimal values (vertical lines). The torque  $0.2T_N$  (crosses),  $0.4T_N$  (triangles),  $0.6T_N$  (squares),  $0.8T_N$  (diamonds), and  $1.0T_N$  (circles).

A simplified structure of the loss-minimizing flux level control augmented with adaptive low-pass filtering of the rotor flux reference is shown in Fig. 5.

The speed controller commands a torque  $T_e$ . The reference for the torque-producing current  $i_{1q,\text{ref}}$  is calculated based on the flux linkage  $\Psi_2$  estimated with a simple first-order model.

The reference  $\Psi_{2,\text{ref}}$  for the rotor flux, corresponds in this setup to the values obtained following the procedure from the previous subsection.

For the laboratory test in Fig. 6, the machine is initialized to operate at a constant speed  $\omega_{2,1}$  and a given load torque  $T_L=0.2T_N$ . At time  $t=0.2s$  a speed ramp to  $\omega_{2,2}$  in the time interval  $[0.2s \ 0.4s]$  is commanded.

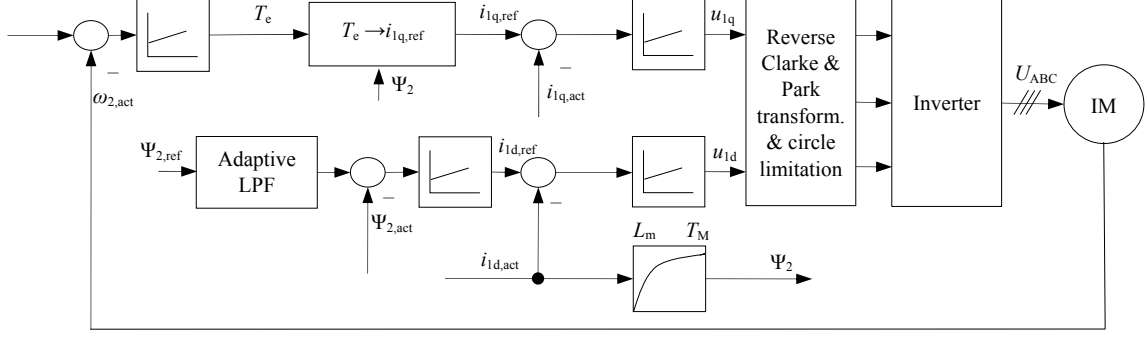


Fig. 5. Control structure

Figure 6 contains six subplots. The uppermost two show the measured data points for the field-producing current  $i_{1d}$  and the torque-producing current  $i_{1q}$ . The next two subplots in the horizontal plane show the stator voltage components  $u_{1d}$  and  $u_{1q}$ . The third line of subplots shows the measured rotor flux  $\Psi_2$ , and power losses  $P_{\text{loss}}$  calculated from the measured stator components, rotor flux, and motor parameters with the help of (10). Finally, the last line shows the measured speed  $\omega_2$  and estimated torque. The same subplots for different operating conditions are shown in Fig. 7.

The moment of inertia  $J$  given in Table 1 is the sum of the moment of inertia of the induction and load motor, the coupling between the two motors, and the torque sensor used in the test bench. The load torque profile is given as follows

$$T_L(t) = \begin{cases} 0.2T_N, & t < 0.2s, t \geq 0.8s \\ 0.4T_N, & 0.2s \leq t < 0.6s \\ 0.6T_N, & 0.6s \leq t < 0.8s \end{cases} \quad (18)$$

The load transition profile from one steady-state operating point to another is assumed to be stepwise.

Due to the low value of the torque at the beginning, the loss-minimizing flux is low as well, and its value corresponds to a well-known result from the steady-state optimization. With the speed increase, the motor torque increases as well, resulting in changes in the loss-minimizing rotor flux trajectories. The change rate of the rotor flux reference is restricted by the bandwidth of the adaptive filtering at the input of the flux controller. A low rotor flux setpoint is used at low torques, and thus, as a rule,

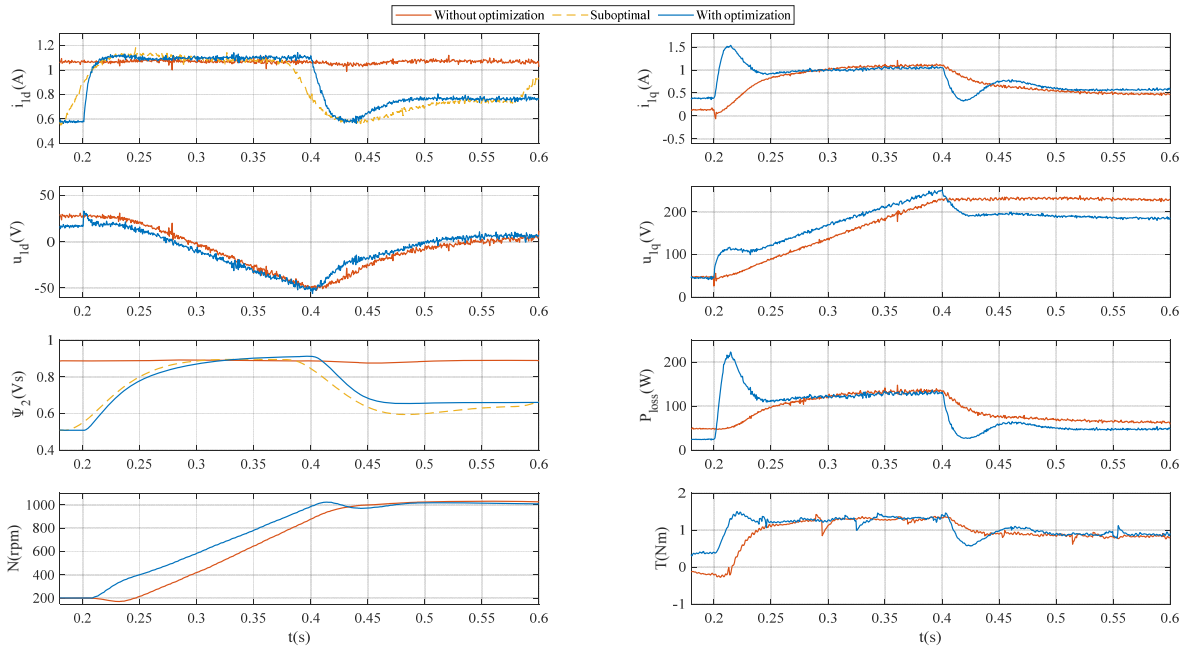
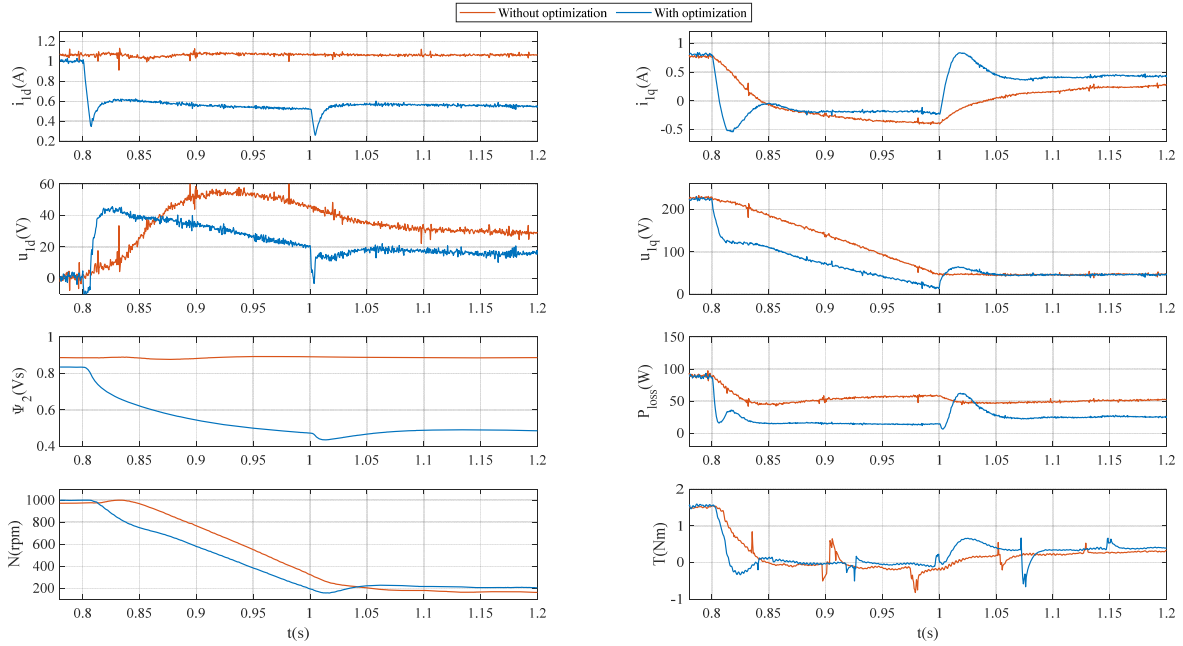
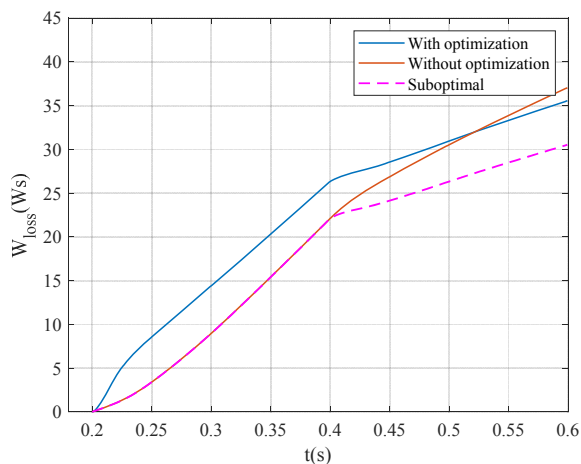


Fig. 6. Experimental results showing speed ramp-up and load torque steps: constant flux control (without optimization), loss-minimizing flux control (with optimization for unknown load changes), for suboptimal case only field-producing current and flux trajectories are shown.



**Fig. 7. Experimental results showing speed ramp-down and load torque steps: constant flux control (without optimization), loss-minimizing flux control (with optimization for unknown load changes).**

increasing the torque takes more time in case of applying loss-minimizing setpoints compared to the case of constant flux operation. Thus, the speed change after the load torque change is more considerable for loss-minimizing control. Nevertheless, the dynamic performance of the proposed law of the rotor flux generation augmented with adaptive low-pass filtering of the flux reference at each sampling step is acceptable for many applications. As for the case of higher dynamic response requirements, the simplest solution consists of the limitation of the bottom terminal value for  $i_{1d}$  setpoint, which leaves a torque reserve. This issue comes from the physical interpretation of the expression for the electromagnetic torque (5). With small  $\Psi_2$



**Fig. 8. Comparison of energy losses.**

the machine is not able to develop the commanded torque setpoint rapidly as a response to a disturbance due to the limitation to the permissible torque-producing current. The maximum length of a stator current phasor is used when massive changes in the flux are demanded. When the commanded speed level is reached, the dynamic torque becomes zero, thus resulting in a new loss-minimizing rotor flux for the steady-state mode of the operation. The abnormal speed

workout of the ramp reference at the beginning for the case of constant flux control might be related to the fact that the load torque was not applied in time before the speed ramp-up.

Figure 7 shows a deceleration process from setpoint  $\omega_{2,2}$  back to  $\omega_{2,1}$ . The machine is

initialized to operate at a constant speed  $\omega_{2,2}$  and a given load torque  $T_L=0.6T_N$ . At time  $t=0.8s$ , a speed ramp to  $\omega_{2,1}$  in the time interval  $[0.8s \ 1s]$  is commanded.

Figure 8 shows the integral of the power losses for the time interval  $[0.2s \ 0.6s]$ . It can be seen that the results for the suggested loss-minimizing technique (with optimization) give much better results compared to the constant flux reference provided that the cycle duration is long enough. Three possible situations shown in Fig. 9 can be detected when dealing with the unknown beforehand load conditions, i.e., a new flux setpoint is commanded simultaneously with the change in torque:



- 1) When the cycle duration is the shortest, the current required for developing the flux in accelerations and decelerations contributes to the power losses so much that the application of loss-minimizing control is no longer actual. The operation under the constant flux is the preferred choice.
- 2) The cycle duration is on the verge of expediency of using any loss-minimizing algorithms since there is no visible effect. It highly depends on load conditions.
- 3) The cycle time is long enough. The total energy losses over the duty cycle under the proposed loss-minimizing law are lower compared to operation under the constant flux.

In order to solve the problem for both case 1 and case 2, a suboptimal approach is proposed. One suggests applying the loss-minimizing reference before the increase of the torque is observed. This means that the knowledge of future torque values is required. Hence, a torque prediction or an appropriately chosen delay of the torque setpoints becomes an actual task for the future developments [23], [24]. It can be roughly said that the suboptimal approach is the combination of the operation under the constant flux and the loss-minimizing flux, as can be seen from Fig. 8.

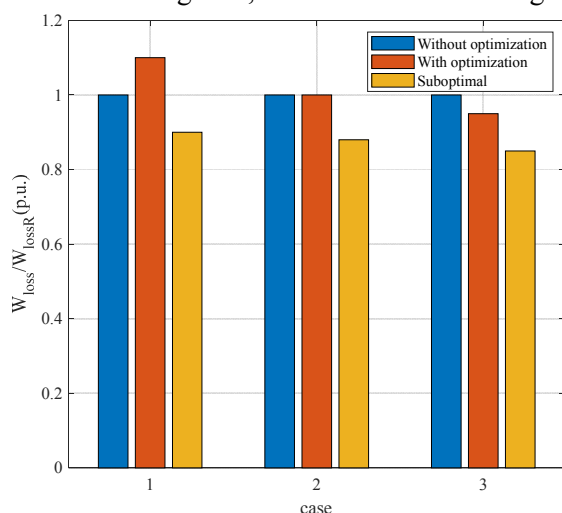


Fig. 9. Energy loss measurement of S5 duty cycles.

## CONCLUSIONS

The current paper presented a law for regulating the coordinates of an electromechanical system, taking into account an energy-efficient algorithm for transferring the system from one operation point to another. In this work, the loss-minimizing trajectories for rotor flux linkage and motor currents were

computed in an online procedure for the unknown torque trajectory and offline for the known in advance load using the adaptive low-pass filtering of the flux reference at each sampling step. The laboratory experiments illustrate that the knowledge about the future torque trajectory is of great asset for a further decrease in the power loss. Furthermore, this knowledge allows to reduce the minimum possible cycle time, at which the expediency of using loss-minimizing control methods remains actual.

## References

- [1] Shibib A., Lorenz L., Ohashi H. ISPSD: 30 Year journey in advancing power semiconductor technology. *2018 IEEE 30th International Symposium on Power Semiconductor Devices and ICs (ISPSD)*, Chicago, IL, 2018, pp. 1-7. doi: 10.1109/ISPSD.2018.8393589.
- [2] Liu G., Li K., Wang Y., Luo H., Luo H. Recent advances and trend of HEV/EV-oriented power semiconductors – an overview. *IET Power Electronics*, 2020, vol. 13, no. 3, pp. 394-404. doi: 10.1049/iet-pel.2019.0401.
- [3] Beshta, O.S. Electric drives adjustment for improvement of energy efficiency of technological processes. *Naukovyi Visnyk Natsionalnoho Hirnychoho Universytetu*, 2012, vol. 4, pp. 98-107.
- [4] Geyer T., Papafotiou G., Morari M. Model Predictive Direct Torque Control—Part I: Concept, Algorithm, and Analysis. *IEEE Transactions on Industrial Electronics*, 2009, vol. 56, no. 6, pp. 1894-1905. doi: 10.1109/TIE.2008.2007030.
- [5] Diachenko G.G., Schullerus G., Dominic A., Aziukovskyi O.O. Real-time loss-minimizing flux level predictive control for closed-cycle operation of field-orientation induction machine drives. *Naukovyi Visnyk Natsionalnoho Hirnychoho Universytetu*, 2020, unpublished.
- [6] Windisch Th., Hofmann W. A Novel Approach to MTPA Tracking Control of AC Drives in Vehicle Propulsion Systems. *IEEE Transactions on Vehicular Technology*, 2018, vol. 67, no. 10, pp. 9294-9302, doi: 10.1109/TVT.2018.2861083.
- [7] Dominic A., Schullerus G., Winter M. Anticipative Flux Trajectories for Dynamic Energy Efficient Operation of Induction Machines. *2020 IEEE Transportation Electrification Conference & Expo (ITEC)*, Chicago, IL, USA, 2020, pp. 1038-1043. doi: 10.1109/ITEC48692.2020.9161450.
- [8] Beshta A., Beshta A., Balakhontsev A., Khudolii A. Performances of Asynchronous Motor within Variable Frequency Drive with Additional Power

- Source Plugged via Combined Converter, 2019 *IEEE 6th International Conference on Energy Smart Systems (ESS)*, Kyiv, Ukraine, 2019, pp. 156-160, doi: 10.1109/ESS.2019.8764192.
- [9] Brix A., Müller V., Hofmann W. Energy Efficient Predictive Rotor Flux Control of Induction Machines in Autonomous Driving Electric Vehicles. *2019 IEEE Transportation Electrification Conference and Expo (ITEC)*, Detroit, MI, USA, 2019, pp. 1-6. doi: 10.1109/ITEC.2019.8790517.
- [10] Bazzi A.M., Krein P.T. Review of methods for real-time loss minimization in induction machines. *IEEE Transactions on Industry Applications*, 2010, vol. 46, no. 6, pp. 2319-2328. doi: 10.1109/TIA.2010.2070475.
- [11] Hannan M.A., Ali J.A., Mohamed A., Hussain A. Optimization techniques to enhance the performance of induction motor drives: A review. *Renewable and Sustainable Energy Reviews*, 2018, vol. 81, pp. 1611-1626. doi: 10.1016/j.rser.2017.05.240.
- [12] Diachenko G.G., Aziukovskiy O.O. Review of methods for energy-efficiency improvement in induction machines. *Naukovyi Visnyk Natsionalnoho Hirnychoho Universytetu*, 2020, no. 1, pp. 80-88, doi: 10.33271/nvngu/2020-1/080.
- [13] Klenke F., Hofmann W. Energy-efficient control of induction motor servo drives with optimized motion and flux trajectories. *Proceedings of the 2011 14th European Conference on Power Electronics and Applications*, Birmingham, 2011, pp. 1-7.
- [14] Stumper J.-F., Dötlinger A., Kennel R. Loss Minimization of Induction Machines in Dynamic Operation. *IEEE Transactions on Energy Conversion*, 2013, vol. 28, no. 3, pp. 726-735. doi: 10.1109/TEC.2013.2262048.
- [15] Plathottam S.J., Salehfar H. Transient energy efficiency analysis of field oriented induction machines. *IEEE Access*, 2017, vol. 5, pp. 20545-20556. doi: 10.1109/ACCESS.2017.2757492.
- [16] Borisevich A., Schullerus G. Energy efficient control of an induction machine under torque step changes, *IEEE Transactions on Energy Conversion*, 2016, vol. 31, no. 4, pp. 1295-1303. doi: 10.1109/TEC.2016.2561307.
- [17] Weiß R., Gensior A. A Model-Based Loss-Reduction Scheme for Transient Operation of Induction Machines. *Proceedings of the 18th European Conference on Power Electronics and Applications*, Karlsruhe, Germany, 2016.
- [18] Qu Z., Ranta M., Hinkkanen M., Luomi J. Loss-minimizing flux level control of induction motor drives. *IEEE Transactions on Industry Applications*, 2012, vol. 48, no. 3, pp. 952-961. doi:10.1109/TIA.2012.2190818.
- [19] Diachenko G., Schullerus G. Simple Dynamic Energy Efficient Field Oriented Control in Induction Motors. *Proceedings of the 18th International Symposium Power Electronics EE2015*, 2015, pp. 1-5.
- [20] Diachenko G.G., Aziukovskiy O.O. A continuous energy-efficiency optimization controller for field-orientation induction motor drives. *System technologies*, 2020, vol. 5, no. 130, pp. 3-14. doi: 10.34185/1562-9945-5-130-2020-01.
- [21] Quang N.P., Dittrich J.-A. Vector Control of Three-Phase AC Machines: *System Development in the Practice*, Berlin: Springer Verlag, 2008.
- [22] Schubert M., Koschik S., De Doncker R. W. Fast optimal efficiency flux control for induction motor drives in electric vehicles considering core losses, main flux saturation and rotor deep bar effect. *2013 Twenty-Eighth Annual IEEE Applied Power Electronics Conference and Exposition (APEC)*, Long Beach, CA, USA, 2013, pp. 811-816. doi:10.1109/APEC.2013.6520303.
- [23] Gao Y., Hendricks L.A., Kuchenbecker K.J., Darrell T. Deep Learning for Tactile Understanding from Visual and Haptic Data. 2015. Available at: <http://arxiv.org/abs/1511.06065> (accessed 30.07.2020).
- [24] Yu J., Weng K., Liang G., Xie G. A vision-based robotic grasping system using deep learning for 3D object recognition and pose estimation. *2013 IEEE International Conference on Robotics and Biomimetics (ROBIO)*, Shenzhen, 2013, pp. 1175-1180. doi: 10.1109/ROBIO.2013.6739623.

#### Information about authors.



Grygorii Diachenko received the B.S. and M.S. degrees in electrical engineering (both with honors in English) from Dnipro University of Technology, Dnipro, Ukraine, in 2013 and 2014, respectively. He is currently pursuing the Ph.D. degree with the Department of Electric Drives.

His research interests include modeling of electromechanical systems, energy-efficient control of electric drives, and learning algorithms for artificial neural networks.

E-mail: [diachenko.g@nmu.one](mailto:diachenko.g@nmu.one)